mReader: Concurrent UHF RFID Tag Reading

Hossein Pirayesh, Shichen Zhang, and Huacheng Zeng
Department of Computer Science and Engineering, Michigan State University

ABSTRACT

UHF RFID tags have been widely used for contactless inventory and tracking applications. One fundamental problem with RFID readers is their limited tag reading rate. Existing RFID readers (e.g., Impinj Speedway) can read about 35 tags per second in a read zone, which is far from enough for many applications. In this paper, we present the first-of-its-kind RFID reader (mReader), which borrows the idea of multi-user MIMO (MU-MIMO) from cellular networks to enable concurrent multi-tag reading in passive RFID systems. mReader is equipped with multiple antennas for implicit beamforming in downlink transmissions. It is enabled by three key techniques: uplink collision recovery, transition-based channel estimation, and zero-overhead channel calibration. In addition, mReader employs a Q-value adaptation algorithm for medium access control to maximize its tag reading rate. We have built a prototype of mReader on USRP X310 and demonstrated for the first time that a two-antenna reader can read two commercial off-the-shelf (COTS) tags simultaneously. Numerical results further show that mReader can improve the tag reading rate by 45% compared to existing RFID readers.

CCS CONCEPTS

• **Hardware** → **Wireless devices**; • **Networks** → **Network protocol design**.

KEYWORDS

GEN2 UHF RFID, multi-tag reading, beamforming, MIMO

ACM Reference Format:

Hossein Pirayesh, Shichen Zhang, and Huacheng Zeng. 2023. mReader: Concurrent UHF RFID Tag Reading. In *International Symposium on Theory, Algorithmic Foundations, and Protocol Design for Mobile Networks and Mobile Computing (MobiHoc '23), October 23–26, 2023, Washington, DC, USA.* ACM, New York, NY, USA, 10 pages. https://doi.org/10.1145/3565287.3610256

1 INTRODUCTION

Passive UHF RFID tags have been used in many sectors of our society, such as warehouses, libraries, retail stores, supply chains, and transportation. Statista forecasts that the RFID technology market revenue worldwide will increase from 20 billion in 2020 to 41 billion in 2025 [21]. In real applications, RFID readers with a fast tag reading rate are always desirable. Such readers will directly enhance the efficiency of tag-intensive RFID systems. However, existing RFID readers have a very limited reading rate. For instance,

MobiHoc '23, October 23–26, 2023, Washington, DC, USA

ACM ISBN 978-1-4503-9926-5/23/10…$15.00
https://doi.org/10.1145/3565287.3610256

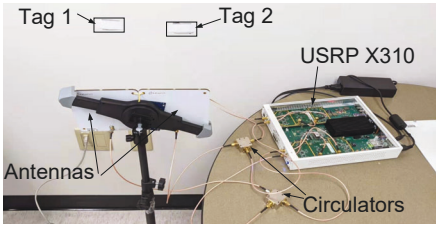

Figure 1: A two-antenna RFID reader (mReader) that can concurrently read two COTS tags.

Impinj Speedway RFID readers can read at most 35 tags/s in a read zone [11], which is far from enough for many applications. This limit stems from the PHY (physical) and MAC (medium access control) layers of RFID communication protocols. At the PHY layer, a reader needs to issue `Select`, `query`, and `ACK` commands in order to obtain `EPC` data from a tag. This process takes about 7 ms in 40 kHz GEN2 UHF RFID systems. It means that the reading rate cannot exceed 150 tags/s at the PHY layer. Moreover, errors may occur during the signal transmission; and tags need to contend for medium access. The coordination of tags' transmission and the management of tag collision will consume a large portion of a reader's airtime, leading to a significantly reduced tag reading rate in real scenarios (e.g., 35 tags/s).

One may think the tag reading rate can be increased by deploying multiple RFID readers on different frequency channels. This does not work because tags would not respond when receiving collided query signals from multiple readers, even if they are on different frequency channels. As such, different approaches have been proposed to increase a reader's tag reading rate, including collision recovery [2, 4, 9, 20], collision management [1, 6, 17, 33], and multi-antenna spatial exploitation [5, 7, 19]. While these approaches indeed improve a reader's tag reading rate to some extent, they have a fundamental limit; namely, a reader can read *at most one* tag in an inventory round (consisting of `Select`, `query`, `RN16`, `ACK`, and `EPC` signalings).

In this paper, we present a new UHF RFID multi-antenna reader (called mReader) that can read multiple commercial off-the-shelf (COTS) tags at the same time and thus has potential to fundamentally increase the tag reading rate. Fig. 1 shows a prototype of mReader. It borrows the idea of multi-user MIMO (MU-MIMO) from cellular networks to enable concurrent multi-tag reading in passive RFID systems. Although MU-MIMO has been well studied in cellular networks, its application and implementation in passive RFID systems face a new challenge in the construction of beamforming filters for concurrent downlink transmission. Specifically, MU-MIMO relies on beamforming (precoding) to pre-mitigate inter-user interference, and the construction of beamforming filters requires downlink channel state information (CSI). However, since RFID tags have very limited communication and computation power, they are incapable of estimating the downlink CSI and reporting it to the reader. To address this challenge, mReader employs implicit

beamforming for downlink transmission by leveraging over-the-air channel reciprocity. Specifically, mReader first estimates uplink CSI based on the received RN16 signals, and then performs a novel RF calibration scheme to infer the downlink CSI for the construction of beamforming filters.

While the idea of implicit beamforming is not new, the estimation of uplink CSI in RFID systems is nontrivial. On one hand, beamforming is sensitive to CSI accuracy; inaccurate CSI is easy to cause interference leakage during the downlink transmission. On the other hand, the reflective signals from RFID tags are very weak, making channel estimation highly susceptible to carrier's phase noise. To combat phase noise, mReader proposes a transition-based channel estimation scheme based on two observations: i) the main energy of phase noise is below 300 kHz, and ii) RFID readers always over sample the signal from tags (e.g., most COST RFID readers use 2 MSps sampling rate for 40 kHz tag signals). Specifically, mReader first decodes the collided bits from tags and then computes the signal transitions corresponding to non-zero bits. The transition bandwidth is selected to 333 kHz (6 signal samples) so as to filter out the main energy of phase noise (300 kHz) while minimizing the effects of thermal noise and circuit imperfections. Finally, the channel estimation problem is formulated to an optimization problem, and its solution can be found using the well-known least-square estimator.

In addition to uplink channel estimation, RF calibration is another key component of implicit beamforming. Although there exist many RF calibration methods, most of them require extra hardware, assistance from external device, or extensive measurement of co-located antenna elements [26]. These approaches are not suitable for RFID readers due to their cost and computation limits. To address this challenge, mReader proposes a *zero-overhead* RF calibration scheme by leveraging its full duplex capability (i.e., transmitting and receiving at the same time). The trick is that mReader manipulates its continuous wave (CW) in the tag-silent period of RFID protocol to estimate RF calibration coefficients. With this RF calibration, mReader is capable of inferring the downlink CSI based on the measured uplink CSI.

Another challenge in the design of mReader lies in the decoding of the collided EPC signals in the uplink when two or more tags concurrently send their EPC signals to mReader. Due to the randomness of RN16 sequence and the heterogeneous modulation of ACK signal, the collided EPC signals are *asynchronous* in time. To decode *asynchronous* EPC signals, mReader takes advantage of the CSI that was estimated based on RN16. It first separates the collided EPC signals in the spatial domain through signal projection, and then employs a voting algorithm to decode the separated EPC bits.

When a large population of tags presents in a read zone, an efficient MAC protocol is critical for a reader to maximize its overall tag reading rate. In UHF RFID systems, a Q value carried by every Query command is used to control a tag's medium access probability. mReader proposes a Q-value adaptation algorithm for tags' medium access control to fully utilize its multi-tag reading capability at the PHY layer. This algorithm maximizes the overall tag reading rate by adaptively increasing the two-tag collision probability without requiring the knowledge about the total number of tags in the read zone.

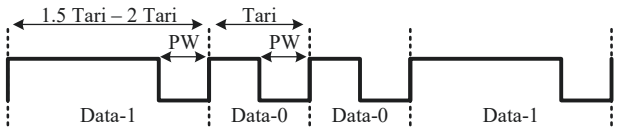

(a) Reader-to-tag communications; PIE encoding.

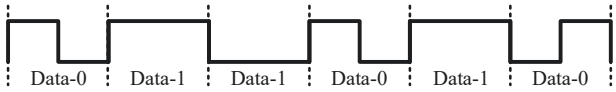

(b) Tag-to-reader communications; FM0 encoding.

Figure 2: RFID data encoding schemes.

We have built a prototype of mReader using USRP X310, RF circulators, and directional antennas as shown in Fig. 1, and demonstrated for the first time that a two-antenna reader can read two commercial tags at the same time. Experimental results show that the success rate of two-tag reading can achieve more than 80% when the two tags are well separated. Due to the limitation of our hardware, emulation was conducted to evaluate the throughput gain of mReader from a system perspective. Numerical results show that mReader can improve the tag reading rate by 45% compared to collision-recovery readers (CR-Reader) and by 126% compared to collision-free readers (CF-Reader).

This paper advances the state-of-the-art as follows.

• It introduces mReader, the *first-of-its-kind* RFID reader that can read multiple tags in an inventory round. mReader is fully compatible with COTS RFID tags.

• It proposes an implicit beamforming scheme for passive RFID systems, featuring phase-noise-resilient channel estimation, zero-overhead RF calibration, and asynchronous EPC signal detection.

• It demonstrates, for the first time, that mReader can read two COTS tags simultaneously *through over-the-air experiments*.

2 PRELIMINARIES

A GEN2 UHF RFID system comprises a reader and battery-free tags, which harvest their operating energy from the reader's CW RF signal and backscatter their information to the reader by switching between reflective and non-reflective antenna states. The goal of RFID communication is for a reader to obtain the electronic product code (EPC) stored on a tag so that it can identify the tag. In what follows, we briefly introduce RFID signal modulation and medium access control.

RFID Signal Modulation: A GEN2 UHF RFID reader operates on 860–960 MHz spectrum bands. In downlink (reader-to-tag) transmissions, the reader uses pulse-interval encoding (PIE) and amplitude shift keying (ASK) modulation. When using PIE, the reader maps data-0 and data-1 to two pulses of different high-value duration, as shown in Fig. 2a. The time duration of data-0 is defined as Tari, which can vary from 6.25μs to 25μs, and the pulsewidth (PW) can vary from max(0.265Tari, 2μs) to 0.525Tari. In uplink (tags-to-reader) transmissions, RFID tags use either FM0 or Miller scheme for data encoding. The FM0 scheme applies a level transition at every symbol boundary as well as the middle of data-0. Fig. 2b shows an example of the FM0 scheme for tag data. Unlike PIE in downlink transmission, FM0 uses time-duration-identical symbols for data-0 and data-1 [14].

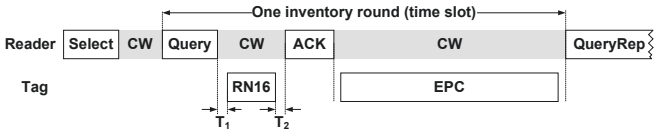

Figure 3: The select and inventory processes.

RFID MAC Protocol: An RFID reader uses a slotted ALOHA MAC mechanism to communicate with tags. Fig. 3 shows the communication between an RFID reader and a tag in order for the reader to obtain the tag' EPC. The reader first selects a tag population using a `Select` command. It then initiates an inventory round by sending a `Query` command. The `Query` command specifies main communication parameters, such as backscatter link frequency, tag-to-reader data encoding scheme (Miller or FM0), and the initial Q value. The Q value determines the number of slots in an inventory round. The reader can further adjust the Q value using `QueryAdjust` command based on the number of detected collisions and no-reply time slots. Upon receiving `Query`/`QueryAdjust` command, each tag picks up a random integer in $[0, 2^Q - 1]$ and uses it as its slot counter. The reader uses `QueryRep` command to let tags countdown their slot counters. When a tag's slot counter reaches zero, it backscatters a 16-bit pseudorandom sequence, known as `RN16`, to the reader. The reader acknowledges its reception of `RN16` by issuing an `ACK` command, which carries the same `RN16` bits. If the tag receives a valid `ACK` command, it will backscatter its `EPC` to the reader; otherwise, the tag will wait for the next `Query`/`QueryAdjust` command to communicate with the reader [10].

Reading Rate Limit: As illustrated in Fig. 3, existing readers can read at most one tag per inventory round. This is a fundamental limit. We note that this limit cannot be overcome by deploying multiple RFID readers on different frequency channels. This is because passive RFID tags cannot differentiate different frequency channels. When a tag receives collided commands on different frequency channels, it cannot function properly.

3 MREADER: AN MU-MIMO RFID READER

Cellular MU-MIMO allows a multi-antenna base station to communicate with multiple single-antenna client users on the same frequency band at the same time. It is considered as one of the most successful technologies for cellular systems as it significantly improves their throughput. mReader was inspired by cellular MU-MIMO. However, RFID is a backscatter communication system, making it non-trivial to design and implement mReader.

RFID MU-MIMO is different from cellular MU-MIMO. In uplink transmissions, cellular MU-MIMO typically employs a special frame structure with orthogonal pilot signals from different users. Such a frame structure allows a base station to estimate the channel between itself and users. However, RFID tags do not have such a capability as they are limited by their communication and computation abilities. Moreover, the reflective signals from tags are very weak and vulnerable to the phase noise of mReader's clock. In downlink transmissions, cellular MU-MIMO requests users to report their estimated channels, and then use the received channels to compute spatial filters for beamforming. RFID systems, however, do not have such luxuries. It is impossible for RFID tags to estimate the downlink channels, let alone channel feedback.

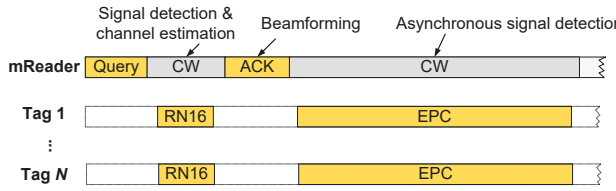

Figure 4: Illustrating RFID MU-MIMO communication between mReader and commercial GEN2 RFID tags.

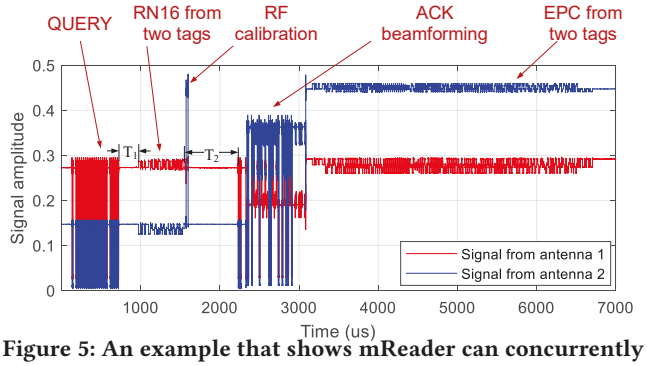

Figure 5: An example that shows mReader can concurrently read two tags. The signals are from our experiments.

mReader addresses these challenges by i) leveraging the special modulation structure of RFID signals to estimate uplink channels and ii) employing implicit beamforming to enable concurrent downlink transmissions. To the end, mReader is capable of concurrently reading multiple COTS RFID tags. In what follows, we focus our design on the two-tag case, and the approach can be extended to a generic case.

3.1 Design Overview

Recall that the communication purpose of an RFID reader is to obtain tags' `EPC` data so as to identify the tagged objects. Fig. 4 depicts the proposed protocol for the communication between mReader and its tags. mReader first broadcasts a `Query` command. Powered by the `CW` signal from mReader, multiple tags respond by sending their `RN16` to mReader. mReader decodes the collided `RN16` signals and estimates channel coefficients between itself and each tag. To acknowledge the tags, mReader performs beamforming to send the decoded `RN16` data back to each individual tag, simultaneously. After being acknowledged, each tag sends out its `EPC`, and mReader decodes the collided `EPC` signals. This process repeats until mReader has read `EPC` data from all tags.

As an example, Fig. 5 shows the received signal from our mReader prototype when it communicates with two tags in one inventory round. It can be clearly seen that the two tags have been successfully triggered to send their `EPC` signals to mReader at the same time. It demonstrates that `RN16` collision recovery, uplink channel estimation, RF calibration, and downlink beamforming are all successful in this instance.

3.2 RN16 Collision Recovery

Referring to Fig. 4, the first question to ask is how to decode the collided `RN16`. Per RFID GEN2 standard, `RN16` consists of a preamble and random payload data. The preamble comprises 12 half-bits, while the random data comprises 34 half-bits (32 half-bits are useful,

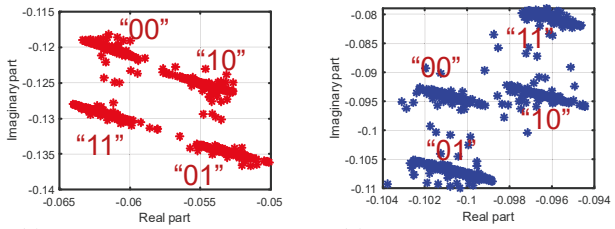

(a) RN16 signal from ant. 1 (b) RN16 signal from ant. 2

Figure 6: RN16 signals received by mReader. The scattering points were caused by signal transition, and the stretched constellation was caused by phase noise.

and two half-bits are dumb). mReader needs to decode the collided RN16 signals so as to acknowledge the tags in the ACK phase. Collision recovery actually has two tasks: i) determine the number of tags, and ii) decode RN16 signal for each tag. A natural approach to carrying out these two tasks is to cluster the received signal samples in the complex plane, as shown in Fig. 6. However, our experiments reveal that using signal amplitude for tag bit clustering yields a similar performance but has a lower computational complexity. This is because the presence of significant phase noise makes it hard to utilize phase information. Fig. 6 shows the constellation of RN16 signal from two tags. It is clear that the constellation is dramatically stretched by phase noise. Therefore, mReader decodes collided RN16 signals using RN16 signal amplitude.

Our algorithm is designed based on the following two observations. First, the RN16 signals from different tags have the same preamble, which consists of 6 tag bits (12 half-bits). The preamble provides the reference signals corresponding to all-zero and all-one cases. Fig. 7 shows the amplitude of the signal from two tags. The signal level of preamble will be used as a reference to determine the number of tags. Second, RFID readers typically use a much higher sampling rate than tag signal baud rate. Following COTS RFID readers, mReader uses 2 MSps sampling rate, i.e., 25× oversampling rate. That said, each RN16 half-bit has 25 samples, which will be used to improve the clustering decision accuracy through a voting mechanism.

Denote $y(i)$ as the ith sample of RN16 signal from mReader's one antenna, where $1 \le i \le 1150$. By leveraging the 6 bits (12 half-bits) of preamble as shown in Fig. 7, we calculate the signal amplitude corresponding to all-zero bits (L_0) and all-one bits (L_1) as follows:

$$L_0 = \frac{1}{12\lfloor\Theta/4\rfloor}\sum_{p=-\lfloor\Theta/4\rfloor}^{\lfloor\Theta/4\rfloor-1}\Big(|y(3\Theta+p)| + |y(5\Theta+p)| + |y(6\Theta+p)| + |y(8\Theta+p)| + |y(9\Theta+p) + y(10\Theta+p)|\Big),$$

$$L_1 = \frac{1}{12\lfloor\Theta/4\rfloor}\sum_{p=-\lfloor\Theta/4\rfloor}^{\lfloor\Theta/4\rfloor-1}\Big(|y(1\Theta+p)| + |y(2\Theta+p)| + |y(4\Theta+p)| + |y(7\Theta+p)| + |y(11\Theta+p)| + |y(12\Theta+p)|\Big),$$

where Θ is the oversampling rate ($\Theta = 25$ for mReader). For a subsequent half-bit, its signal amplitude is computed as follows:

$$L_k = \frac{1}{2\lfloor\Theta/4\rfloor}\sum_{p=-\lfloor\Theta/4\rfloor}^{\lfloor\Theta/4\rfloor-1}|y(k\Theta+p)|,\ k = 13, 14, \cdots, 46.$$

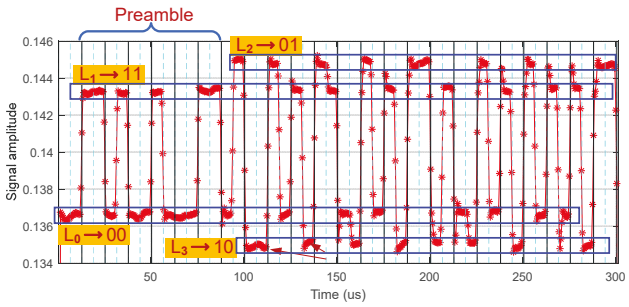

Figure 7: An example of two collided RN16 signals.

where k is the bit index in an RN16 sequence.

Based on the two reference signal levels, we empirically define a threshold ℓ by letting $\ell = |L_0 - L_1|/8$ and create a list $\mathbf{L}$ by initializing it to $\mathbf{L} = [L_0\ L_1]$. We denote L_q as the qth entry in $\mathbf{L}$, and compare tag half-bit L_k to the entries in $\mathbf{L}$. If there is a q so that $|L_q - L_k| \le \ell$, then we assume that L_q and L_k belong to the same cluster and let $g(L_k) = q$. Otherwise, we assume L_k belongs to a new cluster and add L_k to the end of $\mathbf{L}$. At the end of this procedure, the number of tags is equal to $\lfloor\log_2(size(\mathbf{L}))\rfloor$, and the tag half-bits can be decoded based on its corresponding signal level.

Fig. 7 shows an example of the RN16 signal detection in the case with two tags. The preamble reference signal levels are calculated to $L_0 = 0.136$ and $L_1 = 0.143$. The threshold is computed to $\ell = |L_0 - L_1|/8 = 0.00087$. Subsequently, two signal levels are added to the list, which eventually appears to $\mathbf{L} = [L_0, L_1, L_2, L_3] = [0.136, 0.143, 0.145, 0.135]$. Therefore, the number of tags is determined to $\lfloor\log_2(size(\mathbf{L}))\rfloor = 2$, and the corresponding tag half-bits are shown in the figure. We note that the reader cannot distinguish the tags yet, because the RN16 does not carry tag's identification information. Nevertheless, mReader is still capable of sending the RN16 bits back to the corresponding tags using beamforming in the ACK phase.

3.3 Transition-based Channel Estimation

After decoding the collided RN16 signals, mReader estimates the uplink channels from the tags to itself. MU-MIMO beamforming is very sensitive to channel errors, and our experiments indicate that prior methods (e.g., [8, 13]) perform poorly on mReader due to phase noise. To address the phase noise, we propose a transition-based channel estimation scheme for mReader. The key idea behind our scheme is that we utilize the signal transitions, which are caused by tags' state changes, to estimate the channels. Since the transition time duration is much shorter than a tag bit duration, the impact of phase noise can be significantly reduced, making it possible to estimate the channel accurately.

Fig. 8 shows an example of the phase of RN16 signal from our experiments. It is clear that the phase noise of CW is significant. Since the CW is much stronger than the reflective signal from tags, the phase noise decreases the channel estimation accuracy. To reduce the impact of phase noise, we estimate the channels using the transition signal samples as illustrated in Fig. 8. This design is based on two observations. First, the RN16 signal transition at mReader is caused by tag state change (switch on/off). Therefore, the transition signal should carry the full information of channels. Second, the bandwidth of phase noise is much smaller than the sampling rate

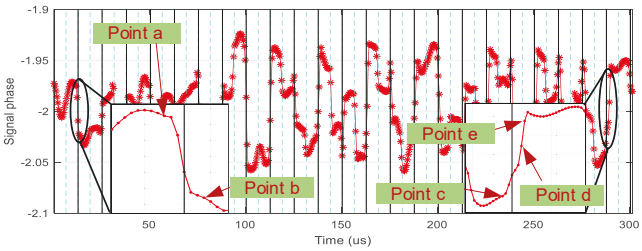

Figure 8: Illustration of signal phase transitions for channel estimation.

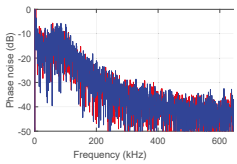

Figure 9: Measured phase noise of CW signal.

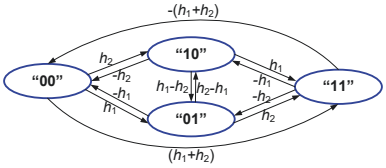

Figure 10: Finite state machine for channel estimation. (states are half-bits of two tags; h_1 and h_2 are channel coefficients.)

(2 MSps for mReader). Fig. 9 shows the spectrum of phase noise. It can be seen that the energy of phase noise concentrates below 300 kHz, which is much smaller than 2 MHz sampling frequency.

Signal Transitions: To estimate channels, we first calculate the signal transitions. Since signal transition occurs at the beginning of each half-bit, we calculate signal transition by:

$$z(k) = y(k\Theta + \theta) - y(k\Theta - \theta), \tag{1}$$

where k is half-bit index, Θ is the oversampling rate (i.e., $\Theta = 25$ for mReader), and $\theta \in \mathbb{N}$ is the offset samples. Note that RN16 sequence has 23 tag bits and therefore it has 46 half-bits in total, i.e., $1 \le k \le 46$.

Fig. 8 illustrates the transition-based channel estimation, where we use the signal change from "point a" to "point b" to infer the channels between mReader and tags. A question to ask is how to choose θ for the signal transition calculation. On one hand, a large θ value will bring phase noise into the transition calculation; on the other hand, a small θ value may incompletely capture the channel information due to the low pass filters within RF chains. To address this problem, we strike a tradeoff between phase noise and filtering. As shown in Fig. 9, the main energy of phase noise is under 300 kHz. Hence, we ensure that the transition bandwidth is greater than 300 kHz. This indicates that the transition can span over $2 \times 10^6/300 \times 10^3 = 6.66$ samples. Therefore, we select $\theta = \lfloor 6.66/2 \rfloor = 3$.

The signal transition calculation in (1) is based on the assumption that the half-bit signals from different tags are well aligned in time. However, for a real low-cost tag, the time duration of its half-bit is susceptible to timing jitters, which may produce meaningless signal transition. To reduce the impact, we propose to exclude the transitions corresponding to large timing jitters. Specifically, we exclude signal transition $z(k)$ for channel estimation if it does not meet the following conditions:

$$\frac{|z(k)|}{A} \ge |y(k\Theta - \theta) - y(k\Theta - \theta - 1)|, \tag{2}$$

$$\frac{|z(k)|}{A} \ge |y(k\Theta + \theta + 1) - y(k\Theta + \theta)|, \tag{3}$$

where we empirically set $A = 8$ and $\theta = 3$ for mReader. Fig. 8 shows a transition with large timing jitter in its second zoom-in subfigure. It can be seen that the gap between "point d" and "point e" is still large. This transition does not meet the condition we defined in (2) and (3). Therefore, we exclude this transition for channel estimation.

Channel Estimation: After computing the signal transitions, we use them to estimate the channels between mReader and tags.

For the two-tag case, Fig. 10 shows the relation between signal transitions and tag channels in a finite state machine. For example, if the tag bits are "00" before transition and "01" after transition, then $z(k) = h_1$; if the tag bits are "01" before transition and "10" after transition, then $z(k) = h_2 - h_1$. In practice, since the tag signal is weak, the observation of signal transitions is susceptible to thermal noise. Therefore, we model the observed signal transition as $z(k) = h(k) + w$, where $h(k)$ is the corresponding channel coefficient as shown in Fig. 10, i.e., $h(k) \in \{h_1, -h_1, h_2, -h_2, h_1 - h_2, h_2 - h_1, h_1 + h_2, -h_1 - h_2\}$, and w is additive white Gaussian noise (AWGN). Then, the channel estimation problem can be formulated as:

$$(h_1, h_2) = \arg\min_{h_1, h_2} \sum_{k=1}^{K} |z(k) - h(k)|^2, \tag{4}$$

where $z(k)$ is the observation of signal transitions, $h(k)$ is a combination of channels shown in Fig. 10, and K is the number of effective signal transition observations (excluding those failed to meet conditions (2) and (3)). Fortunately, the optimal solution to (4) can be found using least-square detector. Denote $\hat{h}_1$ and $\hat{h}_2$ are the channel coefficients between mReader and the two tags. Then, the channels can be estimated by:

$$[\hat{h}_1, \hat{h}_2]^\mathsf{T} = (\mathbf{B}^\mathsf{T}\mathbf{B} + \sigma^2\mathbf{I})^{-1}\mathbf{B}^\mathsf{T}\mathbf{Z}, \tag{5}$$

where $\mathbf{B} = \begin{bmatrix} 1 & 0 & 1 & 1 \\ 0 & 1 & 1 & -1 \end{bmatrix}^\mathsf{T}$ is the constant indication matrix; σ is noise variance, which can be easily estimated using CW signal; $\mathbf{I}$ is a 2×2 identify matrix; $\mathbf{Z} = [z_1, z_2, z_3, z_4]$ with z_p is the average signal transition corresponding to the pth row of $\mathbf{B}$ in Fig. 10. Specifically, z_1 is the average of signal transitions corresponding to edges marked with h_1 and $-h_1$ in Fig. 10; z_2 is the average of signal transitions corresponding to the edges marked with h_2 and $-h_2$; z_3 is the average of signal transitions corresponding to the edges marked with $(h_1 + h_2)$ and $-(h_1 + h_2)$; and z_4 is the average of signal transitions corresponding to the edges marked by $(h_1 - h_2)$ and $(h_2 - h_1)$.

3.4 Zero-Overhead RF Calibration and Beamforming

After decoding RN16, mReader needs to acknowledge those tags. To acknowledge multiple tags simultaneously, mReader employs the beamforming technique, which steers different RN16 signals to their respective tags. The beamforming operation requires downlink channels to construct the precoders. However, the above estimated channels are uplink channels, not downlink channels. While the over-the-air uplink and downlink channels are reciprocal, the responses of Tx and Rx RF chains are not. In what follows, we

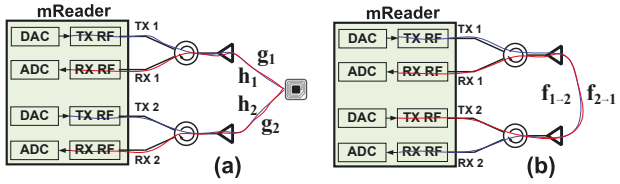

Figure 11: Illustration of our RF calibration method.

first formulate the RF calibration problem and then examine the responses of uplink and downlink channels. Finally, we propose a *zero-overhead* RF calibration method for mReader by leveraging mReader's full-duplex capability.

RF Calibration: Consider the channels between mReader and a tag as shown in Fig. 11(a). Denote h_1 and h_2 are the uplink channels from the tag and mReader's two RF channels. Denote g_1 and g_2 are the downlink channels from mReader's two RF channels to the tag. The objective of RF calibration is to find a coefficient α, so that $\frac{g_1}{g_2} = \alpha \cdot \frac{h_1}{h_2}$. It should be noted that, while mReader is able to measure the uplink channels (h_1 and h_2), it has no way to measure the downlink channels (g_1 and g_2). Mathematically, we have $h_1 = R_1^{\text{ota}} \cdot R_1^{\text{crx}} \cdot R_1^{\text{rxrf}}$ and $h_2 = R_2^{\text{ota}} \cdot R_2^{\text{crx}} \cdot R_2^{\text{rxrf}}$, where R_i^{ota} is the over-the-air channel response between the tag and the ith antenna of mReader, R_i^{crx} is the ith circulator's RX circuit response, and R_i^{rxrf} is the response of mReader's ith RX RF chain. Similarly, we have $g_1 = R_1^{\text{ota}} \cdot R_1^{\text{ctx}} \cdot R_1^{\text{txrf}}$ and $g_2 = R_2^{\text{ota}} \cdot R_2^{\text{ctx}} \cdot R_2^{\text{txrf}}$, where R_i^{ctx} is the ith circulator's TX response, and R_i^{txrf} is the response of mReader's ith TX RF chain. Therefore, the coefficient can be calculated by:

$$\alpha = \frac{g_1 \cdot h_2}{g_2 \cdot h_1} = \frac{R_1^{\text{ctx}} \cdot R_1^{\text{txrf}} \cdot R_2^{\text{crx}} \cdot R_2^{\text{rxrf}}}{R_2^{\text{ctx}} \cdot R_2^{\text{txrf}} \cdot R_1^{\text{crx}} \cdot R_1^{\text{rxrf}}}. \tag{6}$$

Eq. (6) reveals a simple approach to estimate estimate α, which we describe as follows. We first use mReader's Tx1 to send a reference signal and estimate the channel at mReader's RX2, as illustrated in Fig. 11(b). Denote $f_{1\to2}$ as the measured channel. Then, we have $f_{1\to2} = R_1^{\text{ctx}} \cdot R_1^{\text{txrf}} \cdot R^{\text{ota}} \cdot R_2^{\text{crx}} \cdot R_2^{\text{rxrf}}$, where R^{ota} is the OTA channel response. Similarly, denote $f_{2\to1}$ as the measured channel when mReader's TX2 is transmitting and its RX1 is receiving. Then, we have $f_{2\to1} = R_2^{\text{ctx}} \cdot R_2^{\text{txrf}} \cdot R^{\text{ota}} \cdot R_1^{\text{crx}} \cdot R_1^{\text{rxrf}}$. Then, based on (6), we have

$$\alpha = \frac{R_1^{\text{ctx}} \cdot R_1^{\text{txrf}} \cdot R_2^{\text{crx}} \cdot R_2^{\text{rxrf}}}{R_2^{\text{ctx}} \cdot R_2^{\text{txrf}} \cdot R_1^{\text{crx}} \cdot R_1^{\text{rxrf}}} \cdot \frac{R^{\text{ota}}}{R^{\text{ota}}} = \frac{f_{1\to2}}{f_{2\to1}}. \tag{7}$$

Fortunately, the measurement of $f_{1\to2}$ and $f_{2\to1}$ can be easily integrated into the RFID GEN2 protocol while not entailing additional overhead. As shown in Fig. 3, there is a segment of T1 CW signal between Query and RN16 signals. This segment is specified in the standard for tags to prepare their response data (RN16) after receiving the Query command. There is another segment of T2 between RN16 and ACK signals, which is used for the reader to prepare the ACK signal. T1 is 240 μs, and T2 is up to 500 μs when the backscatter link frequency is 40 kHz. While both T1 and T2 are more than enough for RF calibration, mReader uses a small portion of T2 to measure $f_{1\to2}$ and $f_{2\to1}$. As shown in Fig. 5, just after RN16, mReader sends 50 samples (25 μs) of CW signal over TX1 (no transmission on TX2); the received signal at RX2 is $f_{1\to2}(i)$, $i = 1, 2, \cdots, 50$. Then, mReader sends 50 samples (25 μs) of CW signal over TX2 (no transmission on TX1); the received signal at RX1 is $f_{2\to1}(i)$, $i = 1, 2, \cdots, 50$. The RF calibration coefficient is then calculated by $\alpha = \frac{\sum_{i=1}^{50} f_{1\to2}(i)}{\sum_{i=1}^{50} f_{2\to1}(i)}$. Apparently, it does not entail any airtime overhead.

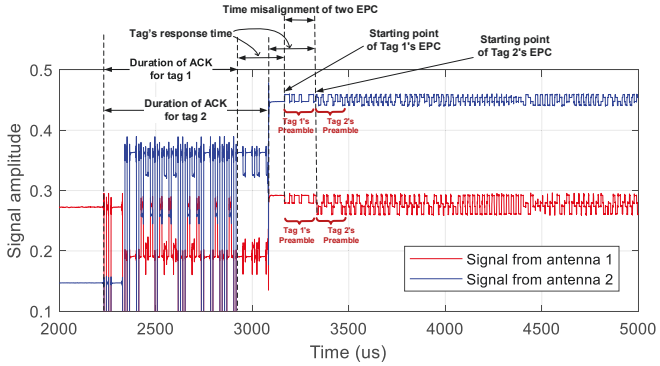

Figure 12: Illustration of time misalignment of EPC signals from two commercial off-the-shelf tags.

Beamforming: After performing RF calibration, mReader employs zero-forcing beamformer to precode the ACK signals. Specifically, mReader performs beamforming as follows:

$$\begin{bmatrix} x_1(i) \\ x_2(i) \end{bmatrix} = \beta \begin{bmatrix} \alpha & 0 \\ 0 & 1 \end{bmatrix} \begin{bmatrix} \hat{h}_{11} & \hat{h}_{12} \\ \hat{h}_{21} & \hat{h}_{22} \end{bmatrix}^{\dagger} \begin{bmatrix} s_1(i) \\ s_2(i) \end{bmatrix}, \tag{8}$$

where $s_m(i)$ is the i signal sample of encoded tag m's RN16 signal, $x_n(i)$ is the ith outgoing signal sample to mReader's nth antenna port, $\hat{h}_{nm}$ is the estimated uplink channel from tag m to mReader's antenna n, α is RF calibration coefficient, β is the scaling factor to meet mReader's transmit power constraint, and $(\cdot)^{\dagger}$ is the pseudo-inverse operator.

3.5 Decoding Asynchronous Collided EPC

After being acknowledged, the tags will concurrently send their EPC signals to mReader, as illustrated in Fig. 4. Now the question is how to decode the collided EPC signals. One may think that the task of decoding the collided EPC signals is the same as the task of decoding the collided RN16 signals. Actually, this is not true. There are two key differences. *First*, the collided EPC signals may be misaligned in time, as illustrated in Fig. 12. This is because the ACK bits are random, and the time durations of data-0 (bit-0) and data-1 (bit-1) are different. In the GEN2 UHF RFID protocol, the ACK phase is to send the decoded RN16 bits back to the tags. RFID readers use PIE for reader-to-tag transmission [10]. In PIE, data-0 is mapped to a pulse-interval signal of Tari. In contract, data-1 is mapped to a pulse-interval signal of η·Tari, where $1.5 \le \eta \le 2$. When the RN16 sequences from the two tags have different numbers of data-1's, the ACK signals for the two tags have different time durations. As a result, the tags start to send their EPC at different time moments, as shown in Fig. 12. *Second*, different tags have slightly different time duration of one bit. This is because tags are low-cost devices having low clock precision. This problem is not significant in the detection of collided RN16 signals, but it is very significant in the detection of collided EPC because EPC is much longer than RN16.

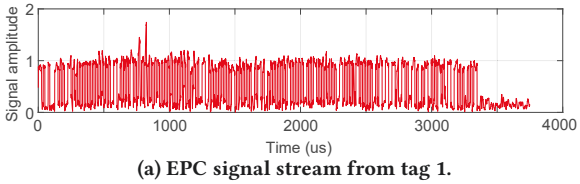

(a) EPC signal stream from tag 1.

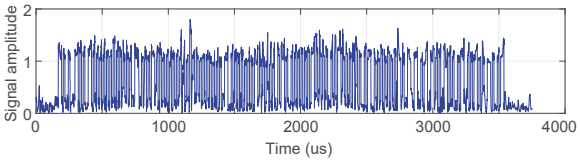

(b) EPC signal stream from tag 2.

Figure 13: Separated EPC signals from experiments.

To address these two challenges, we first perform the spatial separation on the collided EPC signals by taking advantage of the channels estimated in the RN16 phase as follows. $\begin{bmatrix} s_1(i) \\ s_2(i) \end{bmatrix} = \begin{bmatrix} \hat{h}_{11} & \hat{h}_{12} \\ \hat{h}_{21} & \hat{h}_{22} \end{bmatrix}^{\dagger} \begin{bmatrix} y_1(i) \\ y_2(i) \end{bmatrix}$, where $y_n(i)$ is the signal stream from mReader's antenna n, $s_m(i)$ is the separated signal stream from tag m, and $\hat{h}_{mn}$ is the estimated channel based on RN16 as described in Section 3.3. Fig. 13 shows an example of the separated EPC signals. In our experiments, we observed that the two EPC signals can always be well separated. This is because the downlink beamforming and uplink detection are inverse operations due to the channel reciprocity. Successful beamforming in downlink ensures a high probability of EPC signal separation in uplink.

To decode each of the separated EPC signal streams, we first estimate the starting and ending points of EPC over signal stream, based on which we calculate the average time duration of a bit. Then, we take advantage of the oversampling rate (×25) to make decision for each bit using a voting algorithm shown in Alg. 1.

Algorithm 1 A voting algorithm of decoding separated EPC.

Input: Separated EPC signal samples $s_1(i)$ for $1 \le i \le N_1$, and $s_2(i)$ for $1 \le i \le N_2$. K is the number of bits in EPC
Output: Decoded EPC bits $b_1(k)$ and $b_2(k)$

```
for m = 1 : 2 do
    Estimate decision threshold by τ = (1/N_m) Σ_{i=1}^{N_m} |s_m(i)|
    Estimate samples per bit p = N_m / K
    for k = 1 : K do
        vote = 0
        for i = ⌊pk + 1⌋ : ⌊(p + 1)k⌋ do
            vote ← |s_m(i)| ≥ τ ? vote+1 : vote-1
        end for
        b_m(k) = vote > 0 ? 0 : 1
    end for
end for
```

3.6 Q-Value Selection

With the multi-tag reading capability at the PHY layer, we now study the MAC protocol parameters for mReader to optimize its throughput when there are a large population of tags in its read zone. As discussed earlier in Section 2, a reader can control the tags' collision probability by specifying the total number of time slots in a frame using the Q value carried by its Query and QueryAdjust commands. Selecting a proper value for Q is critical for the throughput of a reader. On one hand, a small Q would result in a high collision probability; on the other hand, a large Q would increase the number of no-reply slots. In what follows, we discuss the Q selection in two complementary cases.

Table 1: Optimal Q and throughput (TP) of mReader.

	N=10	N=20	N=40	N=60	N=80	N=100
Optimal Q	4	5	6	6	7	7
TP (tags/reading)	0.86	0.83	0.82	0.84	0.81	0.85
TP gain over CR-Reader	38.5%	38.8%	38.6%	48.8%	38.5%	44.0%
TP gain over CF-Reader	128.6%	126.7%	125.8%	125.9%	125.4%	135.1%

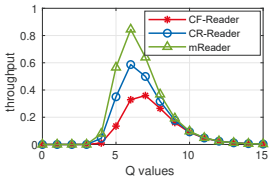

Figure 14: Reader's throughput when it knows N=100.

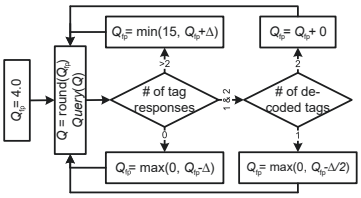

Figure 15: mReader's Q-value adaptation algorithm.

Case 1: Reader knows the number of tags. If a reader knows the total number of tags in its read zone, then the optimum Q-value selection can be formulated as follows:

$$Q_{opt} = \arg\max_{0 \le Q \le 15} \sum_{k=1}^{K} a_k \cdot \binom{N}{k} \left(\frac{1}{2^Q}\right)^k \left(1 - \frac{1}{2^Q}\right)^{N-k}, \tag{9}$$

where N is the total number of tags in the read zone, $(K = 1, a_1 = 1)$ for a collision-avoidance reader (CF-Reader), $(K = 2, a_1 = 1, a_2 = 1)$ for a collision-recovery reader (CR-Reader), and $(K = 2, a_1 = 1, a_2 = 2)$ for mReader. Note that 15 is the upper bound of Q defined in RFID standard [10].

Fig. 14 presents the throughput of CF-Reader, CR-Reader, and mReader when there are $N = 100$ tags in the read zone. It shows that mReader achieves its maximum throughput 0.85 when $Q_{opt} = 6$; the CF-Reader achieves its maximum throughput 0.36 when $Q_{opt} = 7$; and CR-Reader achieves its maximum throughput 0.59 when $Q_{opt} = 6$. Table 1 presents the optimal Q value and the corresponding throughput of the three readers, as well as the gain of mReader compared to CF-Reader and CR-Reader. It is evident that mReader outperforms the other two readers in all cases.

Case 2: Reader does not know the number of tags. In this case, the optimal Q value cannot be directly calculated using (9). We therefore propose a Q-value adaptation algorithm for mReader as shown in Fig. 15. The proposed algorithm starts with an initial floating-point Q value (e.g., $Q_{\text{fp}} = 4$) and updates it based on the perceived tag responses. Specifically, in each inventory round, if the reader observes 0 or 1 tag response, it decreases the Q value so that tags will respond more frequently; if the reader observes more than 2 tag responses, it increases the Q value so that tags will respond less frequently. In GEN2 UHF RFID systems, a reader can send the updated Q value to the tags in each inventory round using Query and QueryAdjust commands. Therefore, the proposed algorithm is backward compatible with off-the-shelf tags.

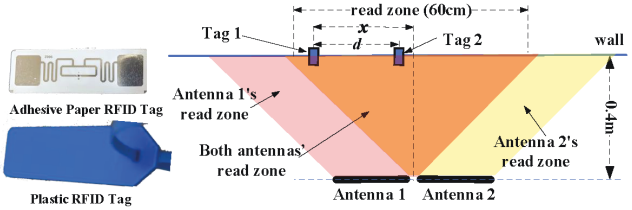

Figure 16: Two COTS tags and experimental setting.

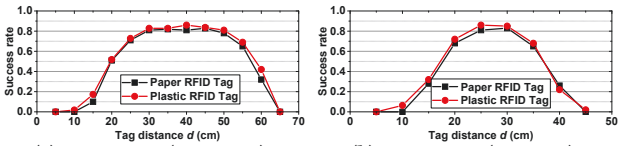

(a) Location 1 (x = 25cm). **(b) Location 2 (x = 5cm).**

Figure 17: mReader's success rate of two-tag reading when the two tags are placed at different locations.

4 PERFORMANCE EVALUATION

The performance of mReader is evaluated through a blend of over-the-air experiments and extensive data-driven emulation.

4.1 Implementation

Hardware: We have built a prototype of mReader as shown in Fig. 1, which comprises one computer, one USRP X310 (with two 40 MHz SBX daughter-boards), two circulators, and two directional antennas. The computer is responsible for digital signal processing, and the USRP X310 is responsible for radio signal transmission and reception. Each circulator offers about 25 dB isolation between the Tx and Rx chains, making it possible for mReader to work in the full-duplex mode. The directional antennas are Keonn Advantenna-p11 UHF RFID antennas, which offer 3.4 dBi gain on 902–928 MHz with about 100° elevation and azimuth beamwidths.

Software: We implement the signal processing modules in C++ using GNU Radio. The challenge in this SDR implementation is to ensure real-time data processing. This is because, referring to the RFID inventory procedure in Fig. 3, a COTS tag must receive ACK within T2 time duration from its RN16 transmission, where T2 must be less than 500 μs. Therefore, mReader must complete the tasks of collision recovery, transition-based channel estimation, and signal beamforming within T2 time duration. This is challenging for SDR implementation because there is a large communication overhead between the computer and USRP X310 (via Ethernet). To address this challenge, we intensively optimize the signal processing modules in GNU Radio by taking advantage of its pipelined block diagram (multi-thread parallel computing). Specifically, we implement the three signal processing modules (collision recovery, channel estimation, and beamforming) using three threads, and reduce the delay of Ethernet connection (between USRP X310 and computer) by setting MTU to a proper value (1000 bytes). By doing so, mReader managed to support real-time communication with COTS tags. Software will be published on GitHub for public access.

4.2 Over-the-Air Experimental Results

We conduct experiments in the scenario as shown in Fig. 16. The two directional antennas are placed side by side, pointing to the same direction. The two tags are attached on the wall, facing to the RFID reader. The distance between mReader's antennas and the wall is about 0.4 m. This distance is limited by the transmit power (about 3 dBm) of mReader. To perform MU-MIMO transmission, the two tags must be within the read zone of both directional antennas, as shown in Fig. 16. Therefore, the distance of interest is about 60 cm on the wall. We placed two tags in this area for our experiments.

Denote d as the distance between the two tags. Denote x as the distance from tag 1 to the central line. We conduct experiments for different values of x and d. For each setting, we perform 15 transmissions, each of which repeats 100 query commands. Here, we set the Q value to 0 in the query command so that both tags will respond with their RN16 at the same time. We measure mReader's success rate of multi-tag reading. Here, a successful case refers to that mReader decodes both tags' EPC in one inventory round, while an unsuccessful case refers to that mReader decodes zero or one tag' EPC in the inventory round. We conducted experiments for two COTS RFID tags. One is Adhesive Paper RFID Tag, and the other is Plastic RFID Tag, as shown in Fig. 16.

As a case study, we place the two tags at the positions of x = 20cm and d = 40cm to examine the uplink and downlink signals. Fig. 5 shows the received signals at mReader. Figs. 7, 12, and 13 show more details of the received signals. It is evident that mReader has successfully obtained both tags' EPC data, meaning that it can read two tags simultaneously.

Fig. 17 presents the experimental results when the two tags are placed at different locations. We have the following observations.

- At both locations, the success rate of multi-tag reading can reach more than 80% (e.g., $30 \le d \le 50$ for the case of $x = 25$). This indicates that multi-tag reading is feasible in real-world RFID systems and has a great potential to improve the tag reading rate.
- At both locations, the success rate of multi-tag reading is low when d is small. The reasons are twofold. First, when the two tags are close to each other (i.e., small d), their signal strengths are similar at mReader, making it hard for mReader to differentiate the signals from the two tags. As a result, mReader has a high probability of failing to decode the collided RN16 signals from the two tags. Second, when d is small, the channel matrix between mReader and two tags tends to be ill-conditioned, making it unsuitable for MU-MIMO communication.
- At both locations, the success rate of multi-tag reading decreases rapidly when d approaches the end of its range (e.g., $50 \le d \le 65$ for the case of x=25). This is because tag 2 is moving out of antenna 1's read zone. At mReader, the received signal from tag 2 becomes weaker as d increases, resulting in a rapid drop of success rate.
- The two types of tags show a consistent profile for their success rates. This indicates that mReader works for diverse tags. It can also be observed that plastic RFID tags offer a slightly better performance than adhesive paper RFID tags. This might be because plastic tags have a larger antenna size and therefore have a higher antenna gain compared to adhesive paper tags.

Based on the observations, we have the following remarks.

Remark 1: Cellular MU-MIMO versus RFID MU-MIMO. Cellular MU-MIMO works in far-field areas. It relies heavily on the rich scattering of wireless environments to realize spatial multiplexing. In contrast, our experiments of RFID MU-MIMO were conducted in a near-field area, where the environment scattering has limited

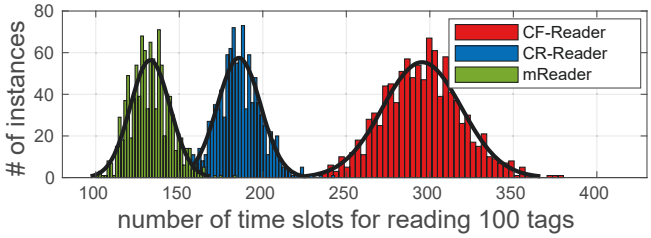

Figure 18: Distribution of the number of time slots required to complete the reading of 100 tags.

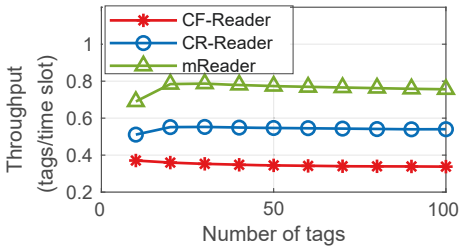

Figure 19: Throughput of three RFID readers.

impact on RFID MU-MIMO. Instead, the non-uniform radiation pattern of RFID antennas plays a key role in the realization of spatial multiplexing.

Remark 2: RFID MU-MIMO in near and far fields. The experimental results show that RFID MU-MIMO works in near-field areas. We expect that RFID MU-MIMO would also work in far-field areas. Commercial RFID readers will not be limited by their transmit power, and their communication range can be extended to several meters. In that case, the tag distance requirement can be easily satisfied.

4.3 Emulation Results: Throughput

Due to the limited reconfigurability of USRP X310's RF chains, the prototyped mReader only allows for a small transmit power (~3dBm) and thus has a short communication range (~0.5m).[1] For this reason, the prototyped mReader cannot be used to conduct large-scale experiments to evaluate its throughput when there are a large number of tags in its read zone. We therefore resort to data-driven emulation.

System Settings: We consider a scenario where mReader does not know the total number of tags in its read zone. It employs the algorithm in Fig. 15 to adapt its Q value for efficient tag reading, with initial $Q_{\text{fp}} = 4$ and $0.1 \leq \Delta \leq 0.5$. For a tag that has already been read (inventoried), mReader issues a `Kill` command in the access process to deactivate this tag, so that it will not respond to the `query` command. Doing so will avoid reading a tag multiple times and therefore accelerate the reading speed. Note that the `Kill` command is supported by GEN2 RFID standard.

Throughput Calculation: The throughput of mReader is calculated by $P = \sum_{k=1}^{K} s_k m_k$, where K is the number of inventory rounds that mReader executes in one second; m_k is the number of responding tags (the tags that send `RN16` after receiving `Query` signal) in the kth inventory round; s_k is mReader's success rate of `EPC` acquisition. In our emulation, $s_k = 1$ when $m_k = 1$; $s_k = 0$ when $m_k > 2$; when $m_k = 2$, we set s_k to 0.8 based on the experimental results in Fig. 17a.

Comparison Baselines: We use CF-Reader and CR-Reader as the comparison baselines. CF-Reader can read a tag only if there is no collision. CR-Reader can recover `RN16` collision of two tags, but it can only obtain one tag's `EPC`. Both CF-Reader and CR-Reader use the Q-value updating algorithm specified in the standard [10]. The throughput of the three readers is calculated by (9).

Average time consumption: We now consider the case where a reader has 100 tags in its read zone. Fig. 18 shows the distribution of the number of required time slots to complete the inventory of all tags. On average, mReader requires 132.5 time slots to complete the tag inventory. In contrast, CF-Reader and CR-Reader require 295.3 and 185.7 time slots, respectively. This indicates that, compared to the state-of-the-art RFID reader (CR-Reader), mReader can shorten the inventory time of 100 tags by 28.6%.

RFID Reader's Throughput: Fig. 19 presents the throughput of the three readers, which is defined as the average number of tags that can be read per time slot (inventory round). On average, the throughput of mReader is 0.77 tags/slot in a tag-dense scenario. In contrast, the throughput of CR-Reader is 0.53 tags/slot, and the throughput of CF-Reader is 0.34 tags/slot. Therefore, mReader can improve the system throughput by 45.2% compared to CR-Reader and 126.4% compared to CF-Reader.

5 RELATED WORK

mReader is the first RFID reader that supports multi-tag reading. We review prior work in the following categories.

Collision Recovery: The basic idea of collision recovery is that a reader attempts to decode collided `RN16` signals from multiple tags so that it can acknowledge one tag for EPC acquisition, thereby turning a collided slot to a successful slot. Many prior works have studied collision recovery in GEN2 RFID systems [2–4, 20, 28, 29]). In [4], Bletsas et al. developed three learning-based algorithms to decode collided RFID signals and derive their error probabilities. In [20], Skyvalakis et al. developed a Viterbi-based signal detection algorithm and a learning-based collision recovery algorithm by leveraging the timing misalignment between collided signals. mReader was designed based on the prior work of collision recovery, but it goes beyond collision recovery. Its main novelty lies in concurrent multi-tag reading.

Multi-Antenna RFID Readers: Multi-antenna RFID readers have been widely deployed for object tracking and localization in RFID systems [12, 15, 18, 22, 24, 25, 27]. Recently, some pioneering works studied multiple antennas for RFID communications. In [5], Bocanegra et al. introduced RFGo, an RFID-based self-checkout system equipped with multiple antennas to enable a reliable and fast check-out experience for customers. The authors proposed a receive space-time diversity technique and an antenna selection mechanism to tackle blind spots and collision problems. In [7], Chen et al. proposed a blind MIMO beamforming scheme to enhance RFID reader range and link quality. In [19], Salah et al. leveraged tags' backscatter link frequency tolerance to differentiate collided signals in frequency, and proposed an antenna selection policy to improve collision recovery performance. All these pioneering works exploited multi-antenna's spatial diversity to improve

[1] This limitation comes from the SDR USRP itself. Practical implementation of mReader does not have this limitation.

the RFID communication reliability. In contrast, mReader exploits multi-antenna's spatial multiplexing to enable concurrent multi-tag reading. Recent work [23] proposed Spotlight, which also considered multiple antennas for concurrent rate-adaptive RFID reading. mReader is advantageous over Spotlight in the two aspects. First, Spotlight needs four antennas to read two tags, but mReader only need to two antennas. Second, Spotlight needs a reference tag for beamforming. In contrast, mReader does not need a reference tag for beamforming.

RFID Collision Management: Another research line to improve tag reading rate is hashing-based collision management. Various hashing-based collision management schemes have been studied for tag inventory and tag search [1, 16, 17, 30–32]. However, most works along this research line are theoretical exploration. mReader differs from and complements this research line.

6 CONCLUSION

In this paper, we presented mReader, the first-of-its-kind RFID reader that supports concurrent multi-tag reading. The design of mReader is underpinned by three key components: uplink collision recovery, transition-based channel estimation, and zero-overhead channel calibration. It also employs a Q-value adaptation algorithm for medium access control to maximize its tag reading rate when there is a large population of tags in its read zone. We have built a prototype of mReader and demonstrated for the first time that a two-antenna reader can read two off-the-shelf tags *simultaneously* via over-the-air experiments. Numerical results show 45% throughput gain of mReader compared to state-of-the-art RFID readers.

ACKNOWLEDGMENT

The authors would like to thank anonymous reviewers for their feedback and suggestions. This work was supported in part by NSF Grants #2225337 and #2100112.

REFERENCES

[1] Zhenlin An, Qiongzheng Lin, Lei Yang, and Wei Lou. 2019. Embracing Tag Collisions: Acquiring Bloom Filters across RFIDs in Physical Layer. In *Proceedings of IEEE Conference on Computer Communications*. 1531–1539.

[2] Christoph Angerer, Robert Langwieser, and Markus Rupp. 2010. RFID reader receivers for physical layer collision recovery. *IEEE Transactions on Communications* 58, 12 (2010), 3526–3537.

[3] Mohammed Benbaghdad, Belkacem Fergani, and Smail Tedjini. 2016. Toward a new PHY layer scheme for decoding tags collision signal in UHF RFID system. *IEEE Communications Letters* 20, 11 (2016), 2233–2236.

[4] Aggelos Bletsas, John Kimionis, Antonis G Dimitriou, and George N Karystinos. 2012. Single-antenna coherent detection of collided FM0 RFID signals. *IEEE Transactions on Communications* 60, 3 (2012), 756–766.

[5] Carlos Bocanegra, Mohammad A Khojastepour, Mustafa Y Arslan, Eugene Chai, Sampath Rangarajan, and Kaushik R Chowdhury. 2020. RFGo: a seamless self-checkout system for apparel stores using RFID. In *Proceedings of the 26th Annual International Conference on Mobile Computing and Networking*. 1–14.

[6] Min Chen, Wen Luo, Zhen Mo, Shigang Chen, and Yuguang Fang. 2013. An efficient tag search protocol in large-scale RFID systems. In *Proceedings of IEEE Conference on Computer Communications*. IEEE, 899–907.

[7] Shaoyuan Chen, Shan Zhong, Siyi Yang, and Xiaodong Wang. 2016. A multi-antenna RFID reader with blind adaptive beamforming. *IEEE Internet of Things Journal* 3, 6 (2016), 986–996.

[8] Hanjun Duan, Haifeng Wu, and Yu Zeng. 2015. Channel estimation for recovery of UHF RFID tag collision on physical layer. In *2015 International Conference on Computer, Information and Telecommunication Systems (CITS)*. IEEE, 1–5.

[9] Karsten Fyhn, Rasmus M Jacobsen, Petar Popovski, Anna Scaglione, and Torben Larsen. 2011. Multipacket reception of passive UHF RFID tags: A communication theoretic approach. *IEEE Transactions on Signal Processing* 59, 9 (2011), 4225–4237.

[10] EPC Global. 2008. EPC radio-frequency identity protocols class-1 generation-2 UHF RFID protocol for communications at 860 MHz–960 MHz. *Version* 1, 0 (2008), 23.

[11] Impinj. 2021. Impinj reader specifications table. Available at: www.shorturl.at/bhzSV [accessed 2021-10-01].

[12] Chengkun Jiang, Yuan He, Xiaolong Zheng, and Yunhao Liu. 2018. Orientation-aware RFID tracking with centimeter-level accuracy. In *17th ACM/IEEE International Conference on Information Processing in Sensor Networks (IPSN)*. IEEE, 290–301.

[13] Jelena Kaitovic, Michal Šimko, Robert Langwieser, and Markus Rupp. 2012. Channel estimation in tag collision scenarios. In *2012 IEEE International Conference on RFID (RFID)*. IEEE, 74–80.

[14] Nikos Kargas, Fanis Mavromatis, and Aggelos Bletsas. 2015. Fully-coherent reader with commodity SDR for Gen2 FM0 and computational RFID. *IEEE Wireless Communications Letters* 4, 6 (2015), 617–620.

[15] Manikanta Kotaru, Pengyu Zhang, and Sachin Katti. 2017. Localizing low-power backscatter tags using commodity WiFi. In *Proceedings of the 13th International Conference on emerging Networking Experiments and Technologies*. 251–262.

[16] Qiongzheng Lin, Lei Yang, Chunhui Duan, and Zhenlin An. 2019. Tash: Toward selective reading as hash primitives for Gen2 RFIDs. *IEEE/ACM Transactions on Networking* 27, 2 (2019), 819–834.

[17] Xiulong Liu, Sheng Chen, Jia Liu, Wenyu Qu, Fengjun Xiao, Alex X Liu, Jiannong Cao, and Jiangchuan Liu. 2020. Fast and accurate detection of unknown tags for RFID systems–hash collisions are desirable. *IEEE/ACM Transactions on Networking* 28, 1 (2020), 126–139.

[18] Yunfei Ma, Xiaonan Hui, and Edwin C Kan. 2016. 3D real-time indoor localization via broadband nonlinear backscatter in passive devices with centimeter precision. In *Proceedings of the 22nd Annual International Conference on Mobile Computing and Networking*. 216–229.

[19] Hamed Salah, Hazem A Ahmed, Joerg Robert, and Albert Heuberger. 2017. Multi-antenna UHF RFID reader utilizing stimulated rate tolerance. *IEEE Journal of Radio Frequency Identification* 1, 2 (2017), 124–134.

[20] Konstantinos Skyvalakis and Aggelos Bletsas. 2021. Asynchronous Reception of 2 RFID Tags. *IEEE Transactions on Communications* (2021).

[21] Statista. 2021. RFID technology market revenue worldwide from 2014 to 2025 by application. Available at: www.shorturl.at/jswM6 [accessed 2021-10-01].

[22] Deepak Vasisht, Guo Zhang, Omid Abari, Hsiao-Ming Lu, Jacob Flanz, and Dina Katabi. 2018. In-body backscatter communication and localization. In *Proceedings of the 2018 Conference of the ACM Special Interest Group on Data Communication*. 132–146.

[23] Ge Wang, Shouqian Shi, Huazhe Wang, Yi Liu, Chen Qian, Cong Zhao, Wei Xi, Han Ding, Zhiping Jiang, and Jizhong Zhao. 2022. Concurrent rate-adaptive reading with passive RFIDs. *IEEE Internet of Things Journal* 10, 1 (2022), 499–511.

[24] Jue Wang, Deepak Vasisht, and Dina Katabi. 2014. RF-IDraw: Virtual touch screen in the air using RF signals. *ACM SIGCOMM Computer Communication Review* 44, 4 (2014), 235–246.

[25] Ju Wang, Jie Xiong, Hongbo Jiang, Xiaojiang Chen, and Dingyi Fang. 2017. D-watch: Embracing "bad" multipaths for device-free localization with cots RFID devices. *IEEE/ACM Transactions on Networking* 25, 6 (2017), 3559–3572.

[26] Hao Wei, Dongming Wang, Huiling Zhu, Jiangzhou Wang, Shaohui Sun, and Xiaohu You. 2015. Mutual coupling calibration for multiuser massive MIMO systems. *IEEE Transactions on Wireless Communications* 15, 1 (2015), 606–619.

[27] Teng Wei and Xinyu Zhang. 2016. Gyro in the air: tracking 3D orientation of batteryless internet-of-things. In *Proceedings of the 22nd Annual International Conference on Mobile Computing and Networking*. 55–68.

[28] Sanika K Wijayasekara, Suvit Nakpeerayuth, Robithoh Annur, Warakorn Srichavengsup, Kumbesan Sandrasegaran, H-Y Hsieh, and Lunchakorn Wutisittikulkij. 2018. A collision resolution algorithm for RFID using modified dynamic tree with Bayesian tag estimation. *IEEE Communications Letters* 22, 11 (2018), 2238–2241.

[29] Haifeng Wu, Xiaogang Wu, Yi Li, and Yu Zeng. 2021. Collision Resolution With FM0 Signal Separation for Short-Range Random Multi-Access Wireless Network. *IEEE Transactions on Signal and Information Processing over Networks* 7 (2021), 438–450.

[30] Lei Yang, Qiongzheng Lin, Chunhui Duan, and Zhenlin An. 2017. Analog on-tag hashing: Towards selective reading as hash primitives in Gen2 RFID systems. In *Proceedings of the 23rd Annual International Conference on Mobile Computing and Networking*. 301–314.

[31] Jihong Yu, Wei Gong, Jiangchuan Liu, and Lin Chen. 2018. Fast and reliable tag search in large-scale RFID systems: A probabilistic tree-based approach. In *Proceedings of IEEE Conference on Computer Communications*. 1133–1141.

[32] Jihong Yu, Wei Gong, Jiangchuan Liu, Lin Chen, and Kehao Wang. 2018. On efficient tree-based tag search in large-scale RFID systems. *IEEE/ACM Transactions on Networking* 27, 1 (2018), 42–55.

[33] Yuanqing Zheng and Mo Li. 2012. Fast tag searching protocol for large-scale RFID systems. *IEEE/ACM Transactions On Networking* 21, 3 (2012), 924–934.